

Bone Microarchitecture and Distal Radius Fracture Pattern Complexity

Anne M. Daniels,^{1,2} Luuk M. A. Theelen,³ Caroline E. Wyers,^{2,4,5} Heinrich M. J. Janzing,¹ Bert van Rietbergen,^{6,7} Lisanne Vranken,^{2,4} Robert Y. van der Velde,^{2,4} Piet P. M. M. Geusens,^{5,9} Sjoerd Kaarsemaker,³ Martijn Poeze,^{2,8} Joop P. vanden Bergh^{2,4,5,9}

¹Department of Surgery, VieCuri Medical Centre, Venlo, The Netherlands, ²NUTRIM School for Nutrition and Translational Research in Metabolism, Maastricht University, Maastricht, The Netherlands, ³Department of Orthopaedic Surgery, VieCuri Medical Centre, Venlo, The Netherlands, ⁴Department of Internal Medicine, VieCuri Medical Centre, Venlo, The Netherlands, ⁵Department of Internal Medicine, Maastricht University, Maastricht, The Netherlands, ⁶Department of Biomedical Engineering, Orthopaedic Biomechanics, Eindhoven University of Technology, Eindhoven, The Netherlands, ⁷Department of Orthopaedic Surgery, Research School CAPHRI, Maastricht University Medical Centre, Maastricht, The Netherlands, ⁸Department of Surgery, Division of Traumasurgery, Maastricht University Medical Centre, Maastricht, The Netherlands, ⁹Faculty of Medicine, Division of Internal Medicine, Hasselt University, Hasselt, Belgium

Received 27 December 2018; accepted 27 March 2019

Published online 24 April 2019 in Wiley Online Library (wileyonlinelibrary.com). DOI 10.1002/jor.24306

ABSTRACT: Distal radius fractures (DRFs) occur in various complexity patterns among patients differing in age, gender, and bone mineral density (BMD). Our aim was to investigate the association of patient characteristics, BMD, bone microarchitecture, and bone strength with the pattern complexity of DRFs. In this study, 251 patients aged 50–90 years with a radiologically confirmed DRF who attended the Fracture Liaison Service of VieCuri Medical Centre, the Netherlands, between November 2013 and June 2016 were included. In all patients fracture risk factors and underlying metabolic disorders were evaluated and BMD measurement with vertebral fractures assessment by dual-energy X-ray absorptiometry was performed. Radiographs of all DRFs were reviewed by two independent investigators to assess fracture pattern complexity according to the AO/OTA classification in extra-articular (A), partially articular (B), and complete articular (C) fractures. For this study, patients with A and C fractures were compared. Seventy-one patients were additionally assessed by high-resolution peripheral quantitative computed tomography. Compared to group A, mean age, the proportion of males, and current smokers were higher in group C, but BMD and prevalent vertebral fractures were not different. In univariate analyses, age, male gender, trabecular area, volumetric BMD (vBMD), and stiffness were associated with type C fractures. In multivariate analyses, only male gender (odds ratio (OR) 8.48 95% confidence interval (CI) 1.75–41.18, $p = 0.008$) and age (OR 1.11 [95% CI 1.03–1.19, $p = 0.007$]) were significantly associated with DRF pattern complexity. In conclusion, our data demonstrate that age and gender, but not body mass index, BMD, bone microarchitecture, or strength were associated with pattern complexity of DRFs. © 2019 The Authors. *Journal of Orthopaedic Research*® Published by Wiley Periodicals, Inc. *J Orthop Res* 37:1690–1697, 2019

Keywords: distal radius fracture (DRF); high-resolution peripheral quantitative CT (HR-pQCT); micro-finite element analyses (micro-FEA); fracture pattern complexity; bone microstructure

Fracture patterns of the distal radius are commonly complex in middle-aged and elderly women, which is related to worse functional outcome. Pattern complexity of DRFs can be assessed using a classification system such as the AO/OTA classification. It is hypothesized that bone microarchitecture and strength are associated with the pattern complexity of the fracture.^{1–8} Decreased bone mineral density (BMD) has been described as a contributor to the peak in incidence rates of distal radius fractures (DRFs) at the age of 50–60 years.^{3,4,7,9–11} Clayton et al.⁶ found a nonsignificant trend toward a higher BMD in partially articular (B) and complete articular (C) fractures compared to complete extra-articular (A) fractures. Several other studies reported no significant difference in mean BMD between extra-articular and complete articular fractures.^{3,7,8} However, assessment of bone microarchitecture and separate

assessment of trabecular and cortical bone is not feasible with bone densitometry. Computed tomography (CT) has been used to assess trabecular and cortical bone, but visualization of trabecular and cortical bone requires spatial resolutions of less than 200 μm .^{12–14} More recently, a noninvasive method for the assessment of bone microarchitecture at the distal radius and tibia using high-resolution peripheral quantitative CT (HR-pQCT) has become available.^{15–18}

To the best of our knowledge, there are no previous studies regarding the association of DRF pattern complexity with bone microarchitecture and strength assessed by HR-pQCT at the distal radius and tibia. In addition, since most studies on DRF pattern complexity contain only female patients, the impact of gender is not yet extensively examined.^{3,6} The aim of this study was to investigate the associations of patient characteristics, BMD (measured by dual-energy X-ray absorptiometry (DXA) and HR-pQCT), bone microarchitecture, and calculated bone strength (by HR-pQCT) with the pattern complexity of DRFs.

METHODS

Study Population

A cross-sectional cohort study (level of evidence: III) was conducted among patients with a recent DRF. All men and

This is an open access article under the terms of the Creative Commons Attribution-NonCommercial-NoDerivs License, which permits use and distribution in any medium, provided the original work is properly cited, the use is non-commercial and no modifications or adaptations are made.

Correspondence to: Anne M. Daniels (T: 31 (0)77 3205555; F: 31 (0)77 3206107; E-mail: adaniels@viecuri.nl)

© 2019 The Authors. *Journal of Orthopaedic Research*® Published by Wiley Periodicals, Inc.

women aged 50–90 years with a clinical fracture who attended the Fracture Liaison Service (FLS) of VieCuri Medical Centre, Venlo, the Netherlands, between November 2013 and June 2016 were identified. Patients with fractures as result of high energy trauma, patients with open fractures, osteomyelitis, and bone metastasis were excluded. A total of 251 patients with a radiologically confirmed DRF were included for this study. At the FLS, patients received a detailed evaluation according to the Dutch guideline for treatment of osteoporosis. The evaluation consisted of a questionnaire assessing risk factors for falls, fracture risk, medical history including medication use, and daily dietary calcium intake. In addition, blood samples were collected to identify metabolic disorders and a DXA measurement with vertebral fractures assessment (VFA) was performed. If indicated, anti-osteoporosis treatment or treatment of newly diagnosed metabolic bone disorders was initiated according to the current guidelines.¹⁹

Of the 251 patients with a DRF included in this study, 71 participated in an observational 3-year follow-up study at the FLS (“Prospective evaluation of bone strength, physical activity, falls, subsequent fractures, and mortality in patients presenting with a recent clinical fracture”). This study is approved by the Medical Ethics Committee (NL 45707.072.13) of Maastricht University. In that study patients consented with HR-pQCT measurements of the distal radius and tibia and the baseline data are used for the HR-pQCT part of the current study.

Assessment of Fracture Pattern Complexity

DRFs were classified based on severity of comminution, displacement, involvement of the radioulnar or radiocarpal joint and associated lesions (e.g., ulnar styloid fracture) according the AO/OTA classification system, which has a strong intra-observer reliability.^{20–22} DRFs were classified into three main types and each main type was then divided into nine subtypes. Type A being extra-articular, type B partial articular, and type C complete articular (Fig. 1). Plain radiographs were used to classify the fractures. Two investigators (A.D. and L.T.) independently classified all fractures by type and subtype according to the AO/OTA classification.²³ In 200 patients, there was agreement between the investigators (A.D. and L.T.). Assessment by a third independent investigator (H.J.) resulted in agreement on another 47 fractures. For the remaining four fractures conformity was reached by all three investigators in a consensus meeting. For this study, type B fractures

were not included in the analysis because we aimed to compare the complete extra-articular fractures (type A) to the complete articular fractures (type C).

DXA

Two-dimensional BMD was measured at the lumbar spine (LS; L1-L4), total hip (TH), and femoral neck (FN) using DXA (Hologic QDR 4500; Hologic Inc., Bedford, MA). BMD measurements were categorized according to the World Health Organization criteria²⁴ based on the lowest *T*-score at the LS, TH, or FN into normal BMD (*T*-score ≥ -1), osteopenia (*T*-score between -1 and -2.5), and osteoporosis (*T*-score ≤ -2.5).

VFA

VFA was performed on the DXA lateral spine images using quantitative morphometric assessment of vertebral height. The method described by Genant et al.²⁵ was used to classify the severity of VF; grade 1 (mild fracture, with vertebral height loss of 20–25%), grade 2 (moderate fracture with height loss of 25–40%), and grade 3 (severe fracture with height loss $> 40\%$).²⁵

HR-pQCT

The nonfractured radius and ipsilateral tibia of the patients were scanned using the second generation HR-pQCT (XtremeCT II; Scanco Medical AG, Brüttisellen, Switzerland). Images were evaluated using the standard manufacturer protocol (effective energy of 68 kVp, tube current of 1470 μ A, and 43 ms integration time).²⁶ A standard phantom was scanned daily for quality control. The patient's forearm and lower leg were placed into an anatomically formed fiber cast to obtain a standardized position. On the basis of a scout view of the forearm and lower leg, the region of interest was determined and a reference line was placed on the joint surface of the distal radius and tibia. The area to be scanned starts 9.0 mm proximally to the reference line and ends 1.2 mm distally to the reference line. Images were reconstructed using an isotropic voxel size of 61 μ m, resulting in 168 consecutive slices. Motion-induced degradation of the images was graded according to the manufacturer's protocol and the method of Pialat et al.²⁷ Scans with grade 1–3, referring to high to moderate quality, were accepted for analysis, scans with grade 4–5 (bad quality) had to be repeated with a maximum of two extra scans.

Images were processed according to the manufacturer's standard protocol.²⁶ The following parameters

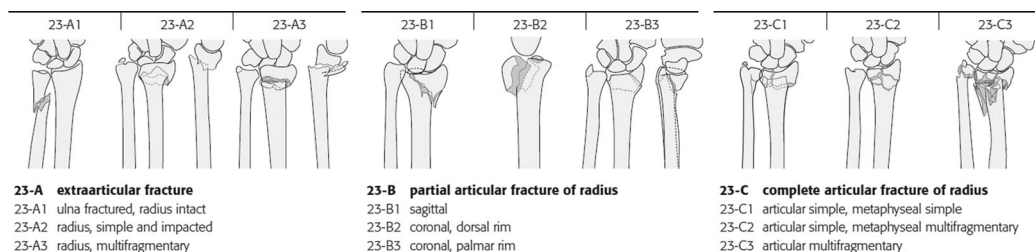


Figure 1. AO/OTA classification for distal radius fractures. Copyright by AO/OTA Foundation, Switzerland.

were analyzed total, trabecular, and cortical bone area (cm^2), volumetric BMD for the total (mgHA/cm^3), trabecular (mgHA/cm^3) and cortical (mgHA/cm^3) compartment, trabecular bone volume fraction, trabecular number (mm^{-1}), trabecular thickness (mm), trabecular separation (mm), cortical thickness (mm), cortical perimeter (mm), cortical porosity (%), and cortical pore diameter (mm). In addition, micro-finite element (micro-FE) analyses were generated by directly converting bone voxels in the segmented image to brick elements.^{28–30} Elements were assigned a Young's modulus of 10 GPa and a Poisson's ratio of 0.3 and for each model, four tests were simulated.³¹ The first load case represented a "high friction" compression test with a prescribed displacement in the axial direction of 1% of the total length, from which the compression stiffness (kN/mm) as well as the estimated strength was calculated.^{32–34} The second load case represented a prescribed rotation of 0.01 rad around the longitudinal axis from which the torsional stiffness (kNmm/rad) was calculated. A third and fourth load case represented a prescribed rotation of 0.01 rad applied around the sagittal and transversal axes, respectively, thus inducing a state of pure bending in two directions, from which the bending stiffness in each direction was calculated. These four load cases were included to test if the fracture type is associated with a reduced stiffness in a specific loading direction.

Statistical Analysis

Data analysis was performed using IBM SPSS Statistics, version 24. Normal distribution was tested using Q-Q plots and the Kolmogorov–Smirnov test. Data are presented as mean with standard deviations (SDs) or as median and interquartile range, depending on their distribution. χ^2 tests and analysis of variance were used to analyze differences between the main types AO/OTA (A/B/C). In further analysis, complete extra-articular fractures (type A) and complete articular fractures (type C) were compared. Independent samples *t* tests were used to compare bone microarchitecture and strength assessed by HR-pQCT between both groups. Logistic regression analysis was used to investigate the independent association between the fracture pattern complexity (type C vs. type A) and baseline characteristics. Univariate analyses were conducted for gender, age, osteopenia, osteoporosis, VFs (grade 2/3), smoking, alcohol use and all standardized scores (*z*-scores) of the HR-pQCT variables for both the HR-pQCT radius group ($N = 55$) and HR-pQCT tibia group ($N = 63$). Multivariate analyses were conducted with adjustment for age and gender for HR-pQCT variables at the distal tibia and radius. The significance level was set as $\alpha = 0.05$.

RESULTS

Patient Characteristics

In this cohort study, 251 patients with a DRF visited the FLS, 38 men (15%) and 213 women (85%) with a mean age of 67 years ($\text{SD} \pm 9$). According to the

AO/OTA classification 131 fractures (52%) were classified as extra-articular (type A) fractures, 36 as partial articular (type B) fractures (14%), and 84 as complete articular (type C) fractures (34%). Overall, there was no difference in patient characteristics between the three groups except for age ($p = 0.034$). On the basis of the *T*-scores, 93 patients (37%) had osteoporosis, 120 (48%) osteopenia, and 38 patients (15%) had a normal BMD (Table 1). Patients in the group with type C fractures ($N = 84$) were older (median age 68.0 [interquartile range (IQR) 14] vs. 66.0 [IQR 16] years, $p = 0.043$) and the proportion of males and was higher (18 (21%) vs. 14 (11%), $p = 0.031$) compared to patients with type A fractures ($N = 131$). There were no differences for body mass index (BMI), BMD, number and severity of VFs, smoking, alcohol intake, and 25(OH) vitamin D.

HR-pQCT Analyses

In a subset of 71 patients, HR-pQCT scans were performed. HR-pQCT of the distal radius was conducted in 63 out of 71 patients; eight patients could not undergo HR-pQCT due to a current or previous bilateral DRF. Of those scans, 61 were graded as high to moderate quality (grade 1–3). Two scans had a poor quality (grade 4/5) and therefore not included in the analysis. HR-pQCT of the tibia was conducted in 71 patients; all scans were graded as high to moderate quality and included in the analysis. Eight patients had a type B DRF and were therefore not included in this analysis. This resulted in a subset of patients 63 patients with type A or C DRFs assessed with HR-pQCT. Patients with type C DRFs ($N = 22$) were significantly older (69 vs. 64 years, $p = 0.009$) and more frequent of male gender (36% vs. 10%, $p = 0.017$) compared to patients with type A DRF ($N = 41$). Exploration of men and women separately revealed that both women ($N = 14$) and men ($N = 8$) with type C DRF were older than those (women $N = 37$, men $N = 4$) with type A DRF (mean difference of 7 years for women and 8 years for men). All other parameters were not different between groups, except for a higher proportion of past smokers in patients with type C DRF (Table S1).

Univariate analyses in the HR-pQCT group are presented in Tables 2 and 3, for distal tibia ($N = 63$) and radius ($N = 55$), respectively. There was a significant association of age, male gender, total area, trabecular area and vBMD, trabecular bone volume fraction, trabecular thickness (only at the distal radius) and cortical perimeter at the distal radius, and tibia with DRF type C versus A. In addition, compression and torsion stiffness at the distal tibia and bending stiffness at the distal radius and tibia were also significantly associated with DRF pattern complexity. After adjustment for age alone, almost all univariate associations for HR-pQCT parameters at the distal tibia and radius remained significant, while after adjustment for gender alone, none of the HR-pQCT parameters was associated with DRF pattern complexity anymore (Tables 2 and 3). Results of the

Table 1. Characteristics of 251 Patients with type A, B, and C Distal Radius Fractures According to the AO/OTA Classification

	AO/OTA A N = 131	AO/OTA B N = 36	AO/OTA C N = 84	p value
Female	117 (89)	30 (83)	66 (79)	N.S.
Age (y)*	66.0 [16]	70.5 [14]	68.0 [14]	0.034
Weight (kg)*	69.9 [23.9]	75.4 [21.7]	72.3 [19.6]	N.S.
Height (m)	1.63 ± 0.07	1.64 ± 0.09	1.64 ± 0.08	N.S.
BMI (kg/m ²)*	25.5 [6.8]	28.0 [7.9]	27.1 [7.3]	N.S.
BMI category				N.S.
<30 kg/m ² (nonobese)	95 (77.9)	21 (63.6)	49 (71.0)	
>30 kg/m ² (obese)	27 (22.1)	12 (36.4)	20 (29.0)	
Bone mineral density				N.S.
Normal BMD	18 (13.7)	4 (11.1)	16 (19.0)	
Osteopenia	66 (50.4)	15 (41.7)	39 (46.4)	
Osteoporosis	47 (35.9)	17 (47.2)	29 (34.5)	
Vertebral fracture assessment				N.S.
No Grade 2/3 Fx	116 (88.5)	29 (80.6)	76 (90.5)	
≥Grade 2/3 Fx	15 (11.5)	7 (19.4)	8 (9.5)	
Smoking				N.S.
Never	49 (38.6)	20 (55.6)	38 (46.3)	
Past smoker	57 (44.9)	12 (33.3)	35 (42.7)	
Current smoker	21 (16.5)	4 (11.1)	9 (11.0)	
Alcohol intake				N.S.
< 1 unit/day	98 (77.2)	30 (85.7)	59 (73.8)	
≥ 1 unit/day	29 (22.8)	5 (14.3)	21 (26.3)	
Calcium intake (mg/day)*	780.0 [320]	785.5 [557]	844.5 [473]	N.S.
25-OH Vitamin D (nmol/l)				N.S.
<30 (deficiency)	14 (10.7)	3 (8.3)	9 (10.7)	
30–50 (insufficiency)	37 (28.2)	10 (27.8)	27 (32.1)	
>50 (sufficiency)	80 (61.1)	23 (63.9)	48 (57.1)	

Data missing: length (26), weight (26), calcium intake (6), alcohol intake (9), smoking (6).

Normally distributed data are presented as mean (SD).

BMD, bone mineral density; BMI, body mass index; Fx, fracture; N.S., not significant.

*Non-normally distributed data are presented as median [interquartile range].

age-adjusted analysis of the female subgroup are analogous to the analyses for the total cohort, with no association of HR-pQCT parameters at the distal tibia ($N = 51$) and distal radius ($N = 43$) (Table S5 and S6).

In the model with adjustment for gender and age, both male gender (OR 8.48 [95% CI 1.75–41.18, $p = 0.008$]) and age (OR per year 1.11 [95% CI 1.03–1.19, $p = 0.007$]) were significantly associated with DRF type C versus A, but no significant associations were found for any HR-pQCT parameters at the tibia or radius.

DISCUSSION

We observed that patients with type C (complete articular) DRFs were significantly older and more frequently of male gender compared to patients with a type A (extra-articular) DRF, but there was no difference in BMI, BMD, number and severity of prevalent VFs, smoking, alcohol intake, and 25(OH) vitamin D levels.

In the unadjusted HR-pQCT analyses, fracture pattern complexity (type C vs. A fractures) was significantly associated with age, male gender, total

trabecular area, vBMD, and stiffness parameters. However, in the fully adjusted model DRF pattern complexity was significantly associated with age and male gender, but not with any of the other parameters. These findings imply that bone characteristics, such as BMD, VF status, bone microarchitecture, and strength are not independently associated with DRF pattern complexity.

In previous studies, it was reported that the prevalence of osteoporosis in patients with DRFs was high compared with prevalence in control subjects and that osteoporosis was a risk factor for DRFs in both men and women.^{4,5} With regard to the severity or complexity of DRFs, literature is sparse, and the methods applied varied. Dhainaut et al.³ reported a weak association between cortical hand BMD by digital X-ray radiogrammetry and increased ulnar variance and dorsal angle, but no association of BMD with the AO scoring system for fracture type. Itoh et al.⁷ reported no significant difference in the mean BMD, measured by DXA at the distal radius and the fracture pattern, which was classified according to a modification of Frykman's system. Although the findings in

Table 2. Associations with Fracture Pattern Complexity (Type C vs. Type A) in 63 Patients With a HR-pQCT at the Distal Tibia

	Unadjusted, OR (CI)	<i>p</i>	Age Adjusted, OR (CI)	<i>p</i>	Gender Adjusted, OR (CI)	<i>p</i>	Age and Gender Adjusted, OR (CI)	<i>p</i>
Gender (M vs. F)	5.29 (1.37–20.36)	0.016	–	–	–	–	8.48 (1.75–41.18)	0.008
Age (per year)	1.09 (1.02–1.16)	0.014	–	–	–	–	1.11 (1.03–1.19)	0.007
Osteopenia	0.38 (0.10–1.50)	0.168	–	–	–	–	–	–
Osteoporosis	0.69 (0.19–2.54)	0.572	–	–	–	–	–	–
Vfx (grade 2/3 vs. no Vfx)	0.60 (0.06–6.17)	0.670	–	–	–	–	–	–
Smoking past	1.75 (0.58–5.32)	0.324	–	–	–	–	–	–
Alcohol (≥ 1 vs. 0/1)	2.40 (0.59–9.76)	0.220	–	–	–	–	–	–
Total area	1.87 (1.07–3.29)	0.028	1.85 (1.02–3.35)	0.042	1.40 (0.70–2.81)	0.344	1.20 (0.56–2.56)	0.637
Trabecular area	1.85 (1.05–3.27)	0.034	1.71 (0.95–3.10)	0.074	1.42 (0.74–2.74)	0.293	1.45 (0.56–2.34)	0.711
Cortical area	1.28 (0.74–2.20)	0.383	1.99 (0.99–4.03)	0.054	0.71 (0.34–1.48)	0.359	1.18 (0.49–2.84)	0.711
Total vBMD	1.09 (0.64–1.86)	0.758	1.40 (0.76–2.56)	0.277	0.88 (0.48–1.59)	0.660	1.14 (0.59–2.20)	0.699
Trabecular vBMD	1.78 (1.01–3.13)	0.047	1.81 (1.00–3.27)	0.050	1.47 (0.80–2.71)	0.212	1.47 (0.76–2.80)	0.237
Cortical vBMD	0.81 (0.47–1.40)	0.452	1.23 (0.63–2.42)	0.549	0.66 (0.36–1.20)	0.170	0.99 (0.49–2.02)	0.993
Trabecular BV fraction	1.80 (1.03–3.14)	0.039	1.80 (1.00–3.22)	0.048	1.51 (0.83–2.74)	0.177	1.48 (0.79–2.77)	0.223
Trabecular thickness	1.15 (0.68–1.95)	0.602	1.13 (0.64–2.00)	0.677	1.23 (0.70–2.15)	0.478	1.22 (0.66–2.27)	0.533
Trabecular separation	0.55 (0.24–1.24)	0.148	0.51 (0.22–1.18)	0.116	0.69 (0.30–1.57)	0.375	0.63 (0.26–1.50)	0.292
Cortical perimeter	1.98 (1.10–3.57)	0.022	1.92 (1.04–3.57)	0.039	1.49 (0.73–3.08)	0.277	1.23 (0.57–2.67)	0.596
Cortical porosity	0.85 (0.48–1.51)	0.583	0.73 (0.38–1.42)	0.353	0.94 (0.51–1.71)	0.828	0.81 (0.40–1.62)	0.547
Cortical thickness	0.93 (0.53–1.60)	0.784	1.33 (0.70–2.50)	0.386	0.70 (0.38–1.31)	0.262	1.02 (0.50–2.05)	0.964
Cortical pore diameter	0.54 (0.27–1.06)	0.073	0.64 (0.32–1.30)	0.214	0.47 (0.22–1.02)	0.056	0.60 (0.28–1.31)	0.199
Torsion stiffness	1.94 (1.11–3.38)	0.020	2.55 (1.27–5.15)	0.009	1.39 (0.55–3.53)	0.490	1.84 (0.65–5.25)	0.252
Compression stiffness	1.78 (1.03–3.09)	0.039	2.29 (1.20–4.39)	0.013	1.23 (0.58–2.61)	0.585	1.60 (0.71–3.60)	0.259
Compression ultimate force	0.52 (0.30–0.89)	0.017	0.54 (0.31–0.96)	0.034	0.68 (0.34–1.36)	0.272	0.89 (0.42–1.91)	0.767
Bending stiffness horizontal	2.08 (1.17–3.70)	0.013	2.60 (1.29–5.24)	0.007	1.66 (0.71–3.87)	0.243	1.96 (0.76–5.01)	0.162
Bending stiffness vertical	1.79 (1.05–3.07)	0.034	2.21 (1.15–4.21)	0.017	1.13 (0.44–2.86)	0.803	1.34 (0.49–3.67)	0.563

ORs for HR-pQCT are presented per standard deviation (SD). CI, confidence interval; OR, odds ratio for DRF type C versus type A; vBMD, volumetric bone mineral density; Vfx, vertebral fracture. Bold indicate significant *p*-values.

Table 3. Associations with Fracture Pattern Complexity (Type C vs. Type A) in 55 Patients With a HR-pQCT at the Distal Radius

	Unadjusted, OR (CI)			Age-Adjusted, OR (CI)			Gender Adjusted, OR (CI)			Age and Gender Adjusted, OR (CI)		
	OR	CI	p	OR	CI	p	OR	CI	p	OR	CI	p
Gender (M vs. F)	5.17	(1.31–20.40)	0.019	–	–	–	–	–	–	8.84	(1.72–45.42)	0.009
Age (per year)	1.08	(1.01–1.16)	0.019	–	–	–	–	–	–	1.11	(1.03–1.19)	0.008
Osteopenia	0.49	(0.12–0.20)	0.316	–	–	–	–	–	–	–	–	–
Osteoporosis	0.62	(0.18–2.42)	0.487	–	–	–	–	–	–	–	–	–
Vfx grade 2/3 vs. no Vfx	0.87	(0.07–10.23)	0.911	–	–	–	–	–	–	–	–	–
Smoking past	1.86	(0.55–6.33)	0.316	–	–	–	–	–	–	–	–	–
Alcohol (≥1 vs. 0/1)	1.47	(0.33–6.47)	0.611	–	–	–	–	–	–	–	–	–
Total area	1.88	(1.07–3.31)	0.029	2.03	(1.10–3.76)	0.025	1.26	(0.48–3.35)	0.638	1.04	(0.36–2.97)	0.949
Trabecular area	1.98	(1.11–3.56)	0.022	1.99	(1.09–3.65)	0.026	1.48	(0.63–3.52)	0.371	1.12	(0.45–2.81)	0.804
Cortical area	1.48	(0.84–2.60)	0.178	1.92	(0.98–3.75)	0.057	0.85	(0.39–1.86)	0.690	1.06	(0.46–2.47)	0.890
Total vBMD	1.06	(0.60–1.85)	0.850	1.34	(0.72–2.49)	0.363	0.88	(0.48–1.63)	0.682	1.12	(0.58–2.18)	0.731
Trabecular vBMD	1.95	(1.05–3.63)	0.036	2.18	(1.12–4.25)	0.021	1.47	(0.71–3.04)	0.295	1.59	(0.75–3.38)	0.226
Cortical vBMD	0.68	(0.37–1.22)	0.197	0.83	(0.43–1.59)	0.573	0.73	(0.39–1.38)	0.333	0.97	(0.49–1.93)	0.937
Trabecular BV fraction	2.15	(1.14–4.04)	0.018	2.33	(1.19–4.59)	0.014	1.68	(0.78–3.54)	0.171	1.69	(0.78–3.67)	0.188
Trabecular thickness	1.98	(1.08–3.62)	0.027	1.77	(0.94–3.34)	0.080	1.65	(0.86–3.15)	0.133	1.28	(0.63–2.61)	0.500
Trabecular separation	0.82	(0.46–1.46)	0.490	0.65	(0.36–1.19)	0.164	1.09	(0.60–2.00)	0.772	0.82	(0.43–1.58)	0.557
Cortical perimeter	1.99	(1.11–3.57)	0.020	1.95	(1.05–3.62)	0.034	1.49	(0.66–3.39)	0.342	1.07	(0.44–2.61)	0.882
Cortical porosity	1.13	(0.63–2.04)	0.683	1.16	(0.60–2.24)	0.663	0.99	(0.52–1.89)	0.978	0.98	(0.46–2.10)	0.958
Cortical thickness	1.12	(0.64–1.95)	0.700	1.49	(0.78–2.86)	0.229	0.86	(0.46–1.61)	0.639	1.11	(0.57–2.19)	0.758
Cortical pore diameter	0.79	(0.40–1.53)	0.474	0.74	(0.34–1.60)	0.443	0.87	(0.43–1.74)	0.686	0.84	(0.36–2.01)	0.701
Torsion stiffness	1.79	(0.99–3.25)	0.056	2.50	(1.19–5.24)	0.015	0.99	(0.36–2.77)	0.998	1.47	(0.41–5.21)	0.552
Compression stiffness	1.50	(0.85–2.64)	0.162	2.11	(1.04–4.29)	0.039	0.91	(0.42–1.96)	0.804	1.24	(0.49–3.13)	0.654
Compression ultimate force	1.55	(0.87–2.74)	0.134	2.22	(1.08–4.56)	0.031	0.95	(0.44–2.07)	0.905	1.33	(0.52–3.46)	0.553
Bending stiffness horizontal	1.54	(0.88–2.69)	0.130	2.08	(1.05–4.10)	0.036	0.74	(0.29–1.91)	0.534	0.96	(0.31–2.98)	0.946
Bending stiffness vertical	2.19	(1.13–4.25)	0.020	3.01	(1.32–6.87)	0.009	1.69	(0.56–5.05)	0.349	2.37	(0.60–9.26)	0.216

ORs for HR-pQCT are presented per standard deviation (SD). CI, confidence interval; OR, odds ratio for DRF type C versus type A; SD, standard deviation; vBMD, volumetric bone mineral density; Vfx, vertebral fracture. Bold indicate significant p-values.

these studies are in line with our study, it is difficult to compare studies due to differences in BMD measurement techniques and location of measurement and DRF classification system.

Clayton et al.⁶ found a trend toward a higher BMD in patients with AO/OTA type B and C fractures compared to type A fractures, which is in contrast to our study. However, they did not directly compare group C versus A and BMD was only measured at the total hip, not at the femoral neck and lumbar spine as we did in our study. In a limited report, de Klerk et al.⁸ found no correlation between the AO-classification of DRFs and BMD, measured at the hip and lumbar spine, which is in line with our findings. Rozental et al.² reported a significantly lower total and trabecular vBMD and trabecular separation, measured by HR-pQCT, at the distal radius and tibia in premenopausal women with a DRF compared to those without a fracture. However, the association of other characteristics, such as prevalent VFs, vitamin D levels, bone microarchitecture, and strength assessed by HR-pQCT, with DRF pattern complexity was not studied up till now.

On the basis of the findings in this study, it is important to note that risk factors known to be associated with fracture risk, such as BMI, osteoporosis, number and severity of prevalent VFs, smoking, and alcohol use are not associated with DRF pattern complexity. In the univariate model, age, male gender, and mainly trabecular micro-architectural parameters as well as compression, torsion, and bending stiffness especially at the distal tibia were associated with DRF pattern complexity. The finding that bone micro-architectural and stiffness parameters were univariate associated with the more complex (type C) DRFs, but not after adjustment for age and gender, can be explained by the fact that men and older patients have larger bones, with greater cortical perimeter, trabecular and total area and trabecular vBMD and higher stiffness.^{35–38}

Our study has limitations. First, we used the AO/OTA classification, which is only one of many fracture classification systems such as the universal system, the Fernandez classification, the Frykman classification, and the Melone classification.^{20,22,39–41} Unfortunately, none of these classification methods has perfect reproducibility.^{10,21,39,40} In contrast to the other classification systems, a strong intra- and inter-observer reliability was reported for the AO/OTA classification when focusing on the main type only (A—extra-articular, B—partly articular, C—complete articular).^{20–22} In line with this, we had a consensus rate of 79.7% after classification by two independent investigators and the distribution of the main types of DRFs correlates with previous published papers.^{3,9,42} Second, we studied a selection of patients that presented at the ED of our hospital with a DRF because assessment of BMD, VFA, and HR-pQCT was only possible in FLS attenders. Third, not all of the patients in our study had a HR-pQCT measurement due to the

retrospective design of our study. However, there was no difference between the HR-pQCT group and non-HR-pQCT group (except for alcohol intake, Table S2); hence, we believe that the results in this study are representative for the total cohort of patients with a DRF. Fourth, the number of patients with type C fractures in the HR-pQCT analyses was relatively low, resulting in large confidence intervals in some of the analyses. In addition, we could only adjust for a limited number of determinants in the multivariate analyses. Fifth, we do not have information on the specific trauma mechanism.

In conclusion, our data demonstrate that age and gender were independently associated with the pattern complexity of DRFs. Other factors known to be associated with fracture risk, such as BMI, osteoporosis, number and severity of prevalent VFs, smoking, and alcohol use are not associated with DRF pattern complexity. This indicates that, besides age and gender, trauma mechanism may also be an important determinant for distal radius fracture pattern complexity.

ACKNOWLEDGMENTS

This study was supported by the VieCuri MC trust for research and innovation. Bert van Rietbergen is a consultant for Scanco Medical AG.

AUTHORS' CONTRIBUTION

A.D. wrote the article. A.D. and C.W. performed the statistical analyses. B.R. conducted all HR-pQCT calculations. A.D., C.W., H.J., B.R., M.P., P.G., and J.B. contributed to the interpretation of the results. A.D., L.T., and H.J. are responsible for the classification of the fractures. L.V. and R.V. implemented all study procedures. M.P., H.J., S.K., P.S., and J.B. supervised the project. All authors discussed the provisional and final results and contributed to the final manuscript. All authors have read and approved the final submitted manuscript.

REFERENCES

- Burghardt AJ, Kazakia GJ, Ramachandran S, Link TM, Majumdar S. 2010. Age- and gender-related differences in the geometric properties and biomechanical significance of intracortical porosity in the distal radius and tibia. *J Bone Miner Res* 25(5):983–993.
- Rozental TD, Deschamps LN, Taylor A, et al. 2013. Premenopausal women with a distal radial fracture have deteriorated trabecular bone density and morphology compared with controls without a fracture. *J Bone Joint Surg Am* 95(7):633–642.
- Dhainaut A, Daibes K, Odinson A, et al. 2014. Exploring the relationship between bone density and severity of distal radius fragility fracture in women. *J Orthop Surg Res* 9:57.
- Oyen J, Brudvik C, Gjesdal CG, et al. 2011. Osteoporosis as a risk factor for distal radial fractures: a case-control study. *J Bone Joint Surg Am* 93(4):348–356.
- Oyen J, Rohde G, Hochberg M, et al. 2011. Low bone mineral density is a significant risk factor for low-energy distal radius fractures in middle-aged and elderly men: a case-control study. *BMC Musculoskelet Disord* 12:67.

6. Clayton RA, Gaston MS, Ralston SH, et al. 2009. Association between decreased bone mineral density and severity of distal radial fractures. *J Bone Joint Surg Am* 91(3):613–619.
7. Itoh S, Tomioka H, Tanaka H, Shinomiya K. 2004. Relationship between bone mineral density of the distal radius and ulna and fracture characteristics. *J Hand Surg Am* 29(1):123–130.
8. de Klerk GJ, Han Hegeman J, Duis HJ. 2013. The relation between AO-classification of distal radial fractures and bone mineral density. *Injury* 44(11):1657–1658.
9. Koo OT, Tan DM, Chong AK. 2013. Distal radius fractures: an epidemiological review. *Orthop Surg* 5(3):209–213.
10. Porrino JA, Maloney E, Scherer K, et al. 2014. Fracture of the distal radius: epidemiology and premanagement radiographic characterization. *AJR Am J Roentgenol* 203(3):551–559.
11. Lotters FJ, van den Bergh JP, de Vries F, et al. 2016. Current and future incidence and costs of osteoporosis-related fractures in the Netherlands: combining claims data with BMD measurements. *Calcif Tissue Int* 98(3):235–243.
12. Prevrhal S, Engelke K, Kalender WA. 1999. Accuracy limits for the determination of cortical width and density: the influence of object size and CT imaging parameters. *Phys Med Biol* 44(3):751–764.
13. Riggs BL, Melton LJ, Robb RA, et al. 2004. Population-based study of age and sex differences in bone volumetric density, size, geometry, and structure at different skeletal sites. *J Bone Miner Res* 19(12):1945–1954.
14. Laib A, Hauselmann HJ, Rueggsegger P. 1998. In vivo high resolution 3D-QCT of the human forearm. *Technol Health Care* 6(5-6):329–337.
15. Petit MA, Beck TJ, Kontulainen SA. 2005. Examining the developing bone: what do we measure and how do we do it? *J Musculoskelet Neuronal Interact* 5(3):213–224.
16. D'Elia G, Caracchini G, Cavalli L, Innocenti P. 2009. Bone fragility and imaging techniques. *Clin Cases Miner Bone Metab* 6(3):234–246.
17. Schneider P, Reiners C, Cointy GR, et al. 2001. Bone quality parameters of the distal radius as assessed by pQCT in normal and fractured women. *Osteoporos Int* 12(8):639–646.
18. Engelke K, Libanati C, Fuerst T, et al. 2013. Advanced CT based in vivo methods for the assessment of bone density, structure, and strength. *Curr Osteoporos Rep* 11(3):246–255.
19. Dutch Institute for Healthcare Improvement CBO. 2011. *Richtlijn Osteoporose en Fractuurpreventie*. Utrecht, the Netherlands: Derde Herziening [Dutch]
20. Lill CA, Goldhahn J, Albrecht A, et al. 2003. Impact of bone density on distal radius fracture patterns and comparison between five different fracture classifications. *J Orthop Trauma* 17(4):271–278.
21. Belloti JC, Tamaoki MJ, Franciozi CE, et al. 2008. Are distal radius fracture classifications reproducible? Intra- and inter-observer agreement. *Sao Paulo Med J* 126(3):180–185.
22. Plant CE, Hickson C, Hedley H, et al. 2015. Is it time to revisit the AO classification of fractures of the distal radius? Inter- and intra-observer reliability of the AO classification. *Bone Joint J* 97-b(6):818–823.
23. Marsh JL, Slongo TF, Agel J, et al. 2007. Fracture and dislocation classification compendium—2007: Orthopaedic Trauma Association classification, database and outcomes committee. *J Orthop Trauma* 21(10 Suppl):S1–133.
24. Kanis JA, Melton LJ, Christiansen C, et al. 1994. The diagnosis of osteoporosis. *J Bone Miner Res* 9(8):1137–1141.
25. Genant HK, Wu CY, van Kuijk C, Nevitt MC. 1993. Vertebral fracture assessment using a semiquantitative technique. *J Bone Miner Res* 8(9):1137–1148.
26. Manske SL, Zhu Y, Sandino C, Boyd SK. 2015. Human trabecular bone microarchitecture can be assessed independently of density with second generation HR-pQCT. *Bone* 79:213–221.
27. Pialat JB, Burghardt AJ, Sode M, et al. 2012. Visual grading of motion induced image degradation in high resolution peripheral computed tomography: impact of image quality on measures of bone density and micro-architecture. *Bone* 50(1):111–118.
28. Agarwal S, Rosete F, Zhang C, et al. 2016. In vivo assessment of bone structure and estimated bone strength by first- and second-generation HR-pQCT. *Osteoporos Int* 27(10):2955–2966.
29. van Rietbergen B, Weinans H, Huiskes R, Odgaard A, et al. 1995. A new method to determine trabecular bone elastic properties and loading using micromechanical finite-element models. *J Biomech* 28(1):69–81.
30. Vrancken L, Wyers CE, van der Velde RY, et al. 2018. Comorbidities and medication use in patients with a recent clinical fracture at the Fracture Liaison Service. *Osteoporos Int* 29(2):397–407.
31. de Jong JJ, Willems PC, Arts JJ, et al. 2014. Assessment of the healing process in distal radius fractures by high resolution peripheral quantitative computed tomography. *Bone* 64:65–74.
32. Pistoia W, van Rietbergen B, Lochmuller EM, et al. 2004. Image-based micro-finite-element modeling for improved distal radius strength diagnosis: moving from bench to bedside. *J Clin Densitom* 7(2):153–160.
33. Mueller TL, Christen D, Sandercott S, et al. 2011. Computational finite element bone mechanics accurately predicts mechanical competence in the human radius of an elderly population. *Bone* 48(6):1232–1238.
34. Hosseini HS, Dunki A, Fabech J, et al. 2017. Fast estimation of Colles' fracture load of the distal section of the radius by homogenized finite element analysis based on HR-pQCT. *Bone* 97:65–75.
35. Seeman E. 2008. Bone quality: the material and structural basis of bone strength. *J Bone Miner Metab* 26(1):1–8.
36. Ruff CB, Hayes WC. 1988. Sex differences in age-related remodeling of the femur and tibia. *J Orthop Res* 6(6):886–896.
37. Duan Y, Turner CH, Kim BT, Seeman E. 2001. Sexual dimorphism in vertebral fragility is more the result of gender differences in age-related bone gain than bone loss. *J Bone Miner Res* 16(12):2267–2275.
38. Wang XF, Duan Y, Beck TJ, Seeman E. 2005. Varying contributions of growth and ageing to racial and sex differences in femoral neck structure and strength in old age. *Bone* 36(6):978–986.
39. Arealis G, Galanopoulos I, Nikolaou VS, et al. 2014. Does the CT improve inter- and intra-observer agreement for the AO, Fernandez and Universal classification systems for distal radius fractures? *Injury* 45(10):1579–1584.
40. Andersen DJ, Blair WF, Steyers CM, et al. 1996. Classification of distal radius fractures: an analysis of interobserver reliability and intraobserver reproducibility. *J Hand Surg Am* 21(4):574–582.
41. Ferrero A, Garavaglia G, Gehri R, et al. 2011. Analysis of the inter- and intra-observer agreement in radiographic evaluation of wrist fractures using the multimedia messaging service. *Hand (N Y)* 6(4):384–389.
42. Jayakumar P, Teunis T, Gimenez BB, et al. 2017. AO distal radius fracture classification: global perspective on observer agreement. *J Wrist Surg* 6(1):46–53.

SUPPORTING INFORMATION

Additional supporting information may be found in the online version of this article.